

This is an Open Access document downloaded from ORCA, Cardiff University's institutional repository:<https://orca.cardiff.ac.uk/id/eprint/108292/>

This is the author's version of a work that was submitted to / accepted for publication.

Citation for final published version:

Yu, Siyu, Yang, Nianjun, Vogel, Michael, Mandal, Soumen , Williams, Oliver A. , Jiang, Siyu, Schönherr, Holger, Yang, Bing and Jiang, Xin 2018. Battery-like supercapacitors from vertically aligned carbon nanofiber coated diamond: design and demonstrator. *Advanced Energy Materials* 8 (12) , 1702947.
10.1002/aenm.201702947

Publishers page: <http://dx.doi.org/10.1002/aenm.201702947>

Please note:

Changes made as a result of publishing processes such as copy-editing, formatting and page numbers may not be reflected in this version. For the definitive version of this publication, please refer to the published source. You are advised to consult the publisher's version if you wish to cite this paper.

This version is being made available in accordance with publisher policies. See <http://orca.cf.ac.uk/policies.html> for usage policies. Copyright and moral rights for publications made available in ORCA are retained by the copyright holders.



Supporting Information

Battery-like Supercapacitors from Vertically Aligned Carbon Nanofibers Coated Diamond: Design and Demonstrator

Siyu Yu, Nianjun Yang, Michael Vogel, Soumen Mandal, Oliver A. Williams, Siyu Jiang,
Holger Schönherr, Bing Yang, and Xin Jiang**

S. Yu, Dr. N. Yang, Dr. M. Vogel, Prof. X. Jiang

Institute of Materials Engineering, University of Siegen, 57076 Siegen, Germany

E-mail: nianjun.yang@uni-siegen.de, xin.jiang@uni-siegen.de

Dr. S. Mandal, Prof. O. A. Williams

School of Physics and Astronomy, Cardiff University, Cardiff CF24 3AA, UK

S. Jiang, Prof. H. Schönherr

Physical Chemistry I, Department of Chemistry and Biology & Research Center of Micro and Nanochemistry and Engineering (Cμ), University of Siegen, 57076 Siegen, Germany

Dr. B. Yang

Shenyang National Laboratory for Materials Science, Institute of Metal Research (IMR), Chinese Academy of Sciences (CAS), No.72 Wenhua Road, Shenyang 110016 China

Experimental

Figures

Tables

Supporting references

Experimental

The growth of CNFs was also performed using Cu particles as the catalysts. Cu particles were obtained through thermal annealing of the sputtered copper films under the conditions of an annealing temperature of 500 °C, a pressure of about 5×10^{-2} mbar, and an annealing time of 60 min. SEM images of these annealed Cu films are shown in **Figure S5**. During the thermal treatment, Cu films split apart to form islands. Some of these islands further aggregate into separate particles. For Cu films with different sputtering times ($t_{Cu,s}$) from 15 to 60 s, the converged Cu particles feature larger sizes and higher densities. Both are varied as a function of $t_{Cu,s}$. For Cu films with $t_{Cu,s}$ from 90 to 120 s, the disintegrated films are not completely converted into drop-shaped particles. This is due to the increased thicknesses of copper films and insufficient annealing time.

SEM images of CNFs grown on these annealed Cu films are presented in **Figure S6** (for $t_{Cu,s}$ from 15, 30, 60, 90, and 120 s). The inset images show the cross sections of the related films. Vertically aligned CNFs are gained with $t_{Cu,s}$ of 90 and 120 s. This is attributed to the nearly continuous dispersion of Cu fragments, resulting in analogous growth phenomenon as that without annealing of the Cu films (WOA). For the CNFs/BDD hybrid films with $t_{Cu,s}$ from 15 to 60 s, disordered CNFs with different dimensions are obtained, closely associated with the distribution and size of Cu particles. The thicknesses of these CNF films with annealing (WA) of the Cu films are about 2.2, 2.5, 3.0, 3.2, and 3.3 μm for $t_{Cu,s}$ of 15, 30, 60, 90, and 120s, respectively. These values are slightly smaller than those CNF films WOA. The difference is originated from the influence of varied sizes of Cu catalysts on the growth rates of the CNFs.^[S1]

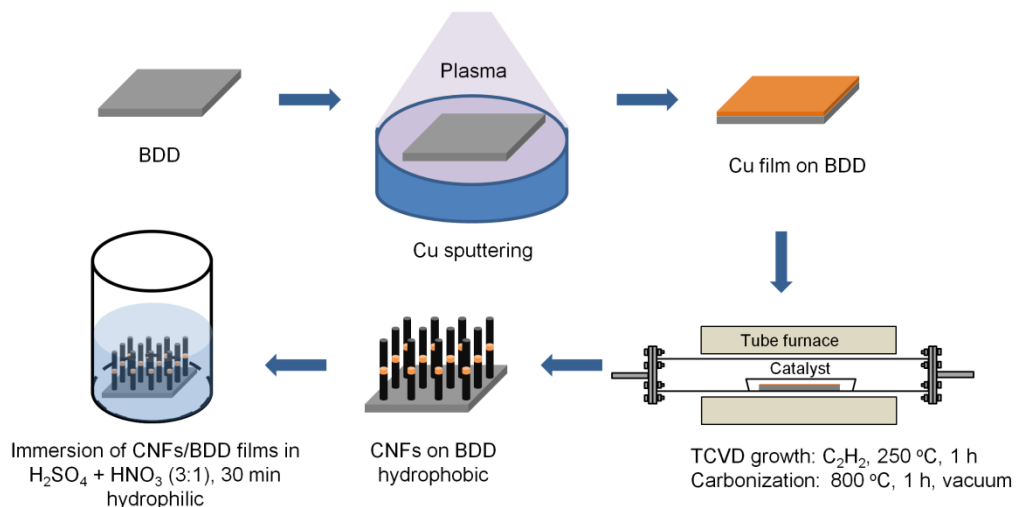
Figures

Figure S1. Schematic plots of the synthesis of the CNFs/BDD hybrid films using a thermal chemical vapor deposition (TCVD) technique.

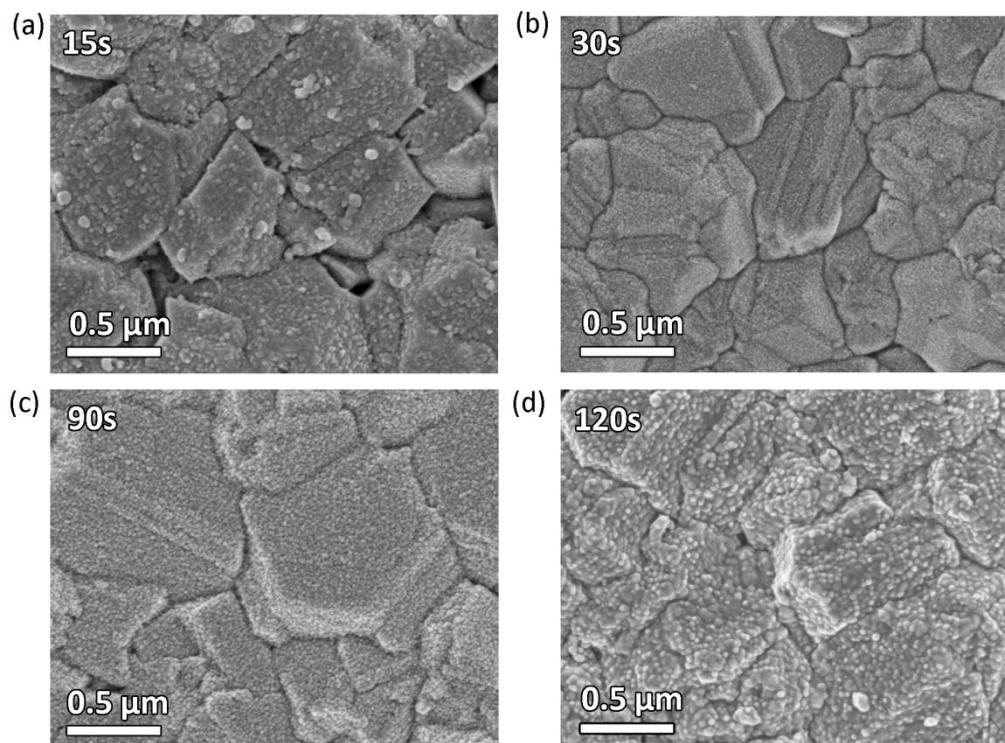


Figure S2. SEM images of Cu films on BDD with $t_{\text{Cu},\text{s}}$ of (a) 15, (b) 30, (c) 90, and (d) 120 s.

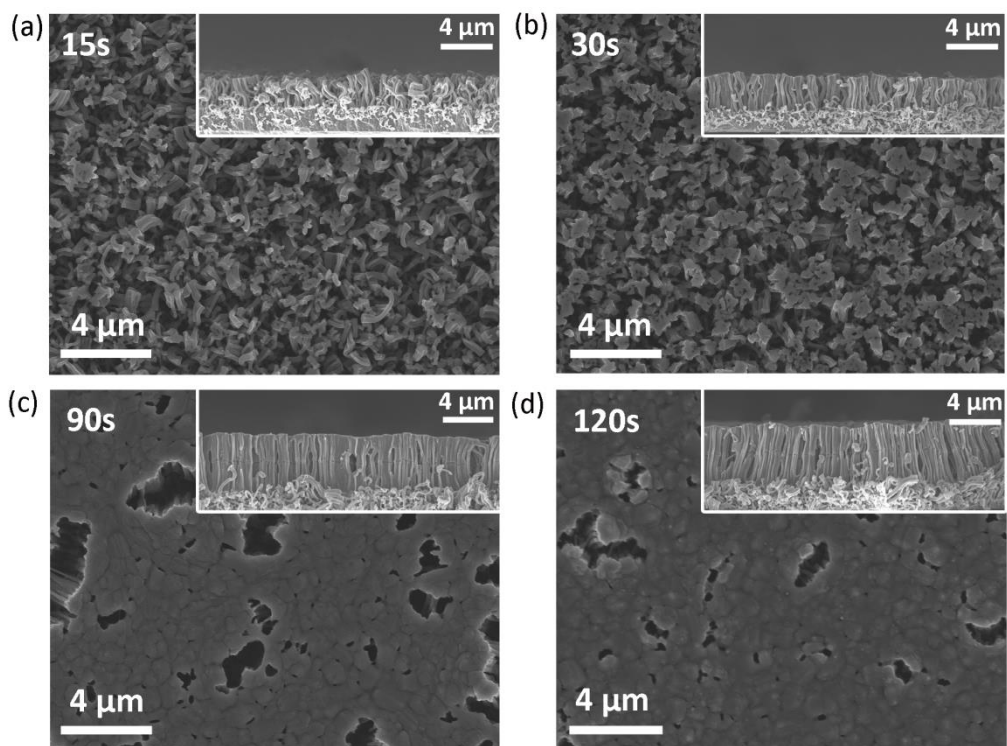


Figure S3. SEM images of the CNFs on BDD with $t_{\text{Cu,s}}$ of (a) 15, (b) 30, (c) 90, and (d) 120 s.

The insets show the SEM cross section of the films.

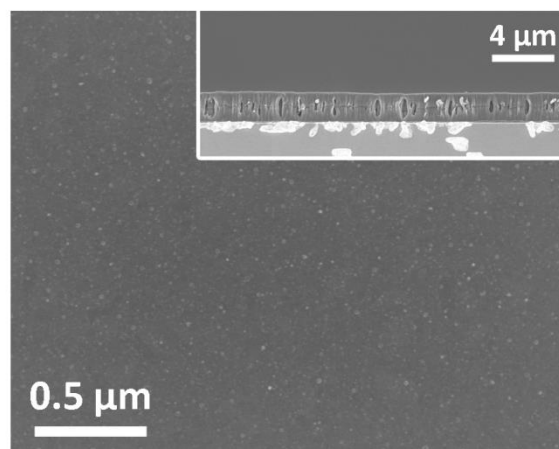


Figure S4. SEM image of a CNFs film grown on a smooth Si substrate with $t_{\text{Cu,s}}$ of 60 s,

WOA. The inset shows its cross section.

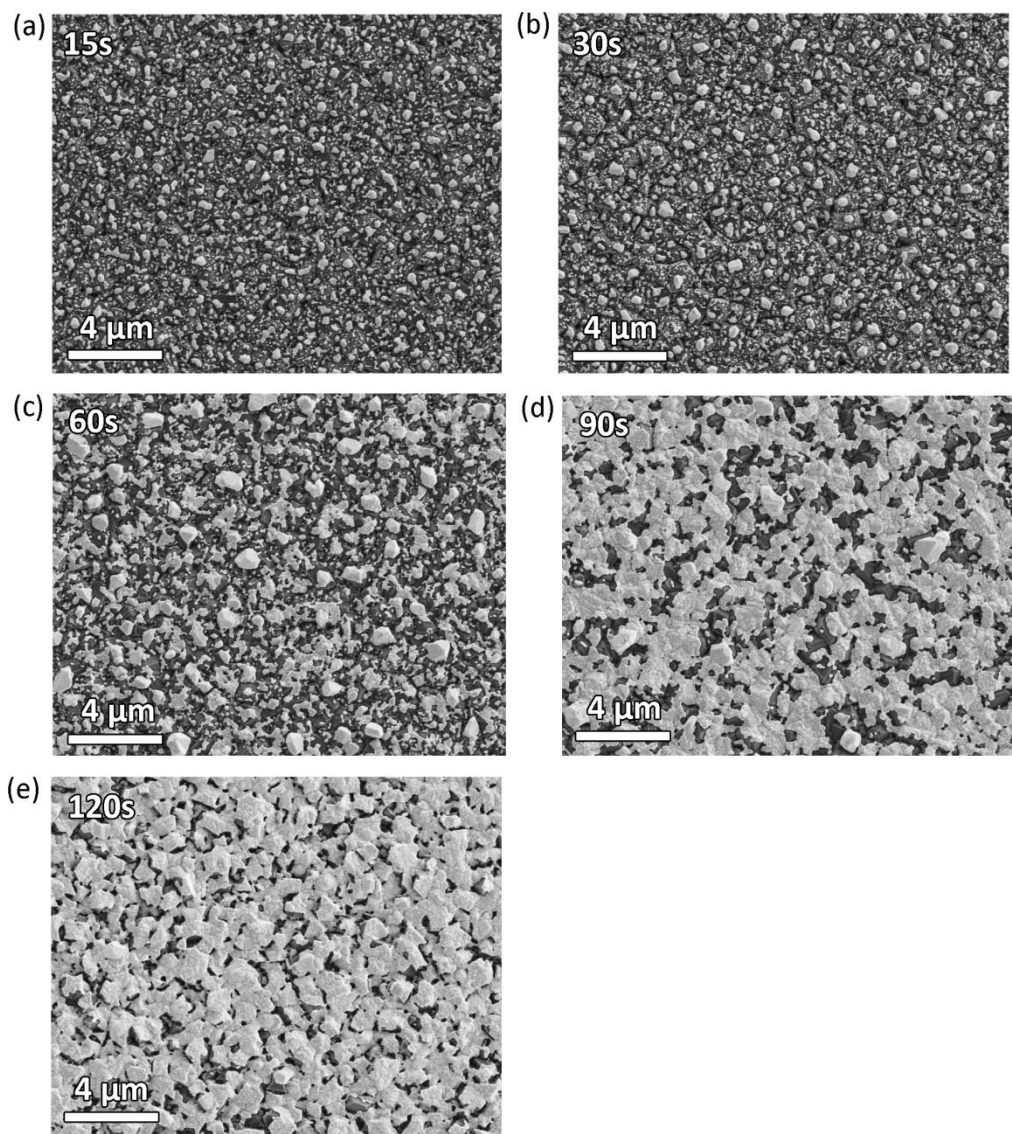


Figure S5. SEM images of Cu films with $t_{\text{Cu,s}}$ of (a) 15, (b) 30, (c) 60, (d) 90, and (e) 120 s after annealing at 500 °C for 1 h in vacuum.

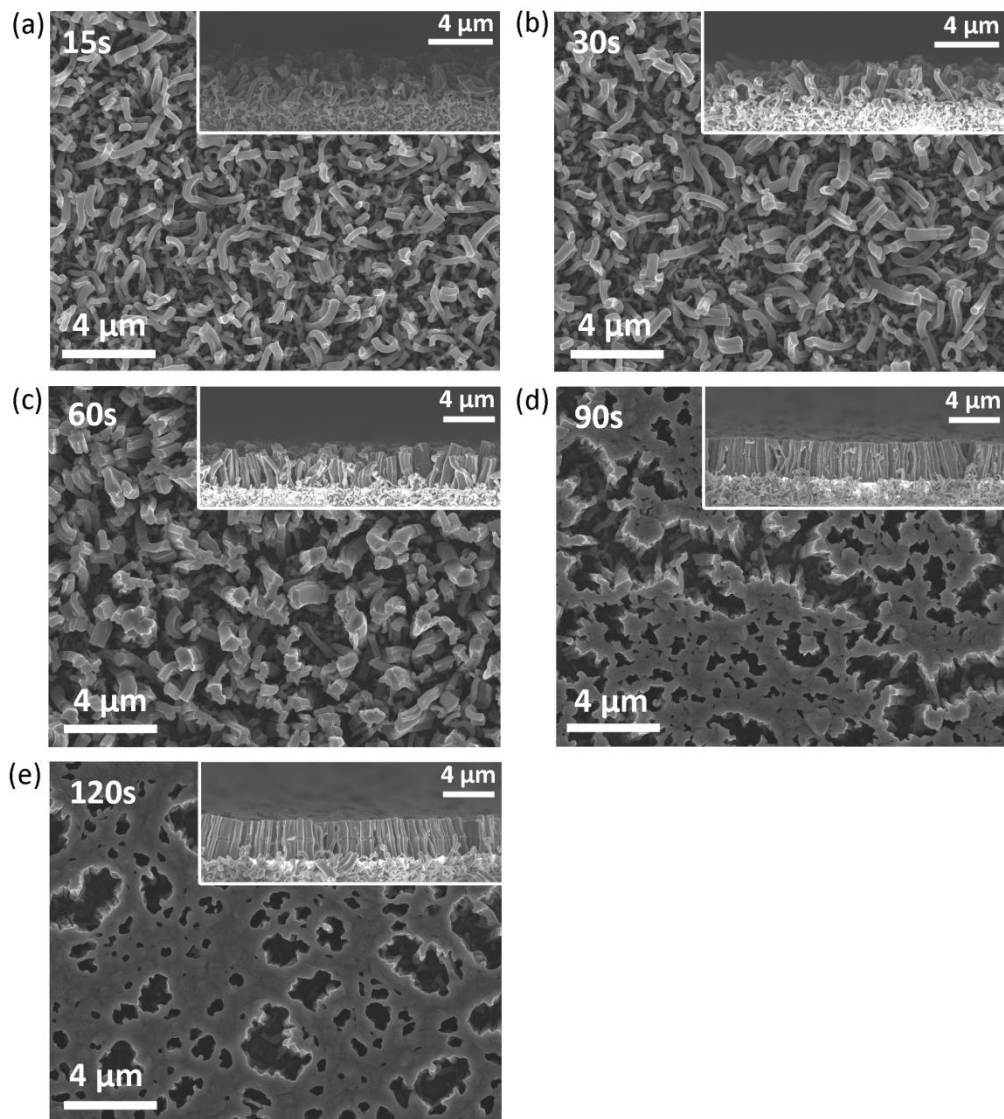


Figure S6. SEM images of the CNFs grown on BDD after the annealing of Cu films with $t_{\text{Cu,s}}$ of (a) 15, (b) 30, (c) 60, (d) 90, and (e) 120 s. The insets show the cross sections.

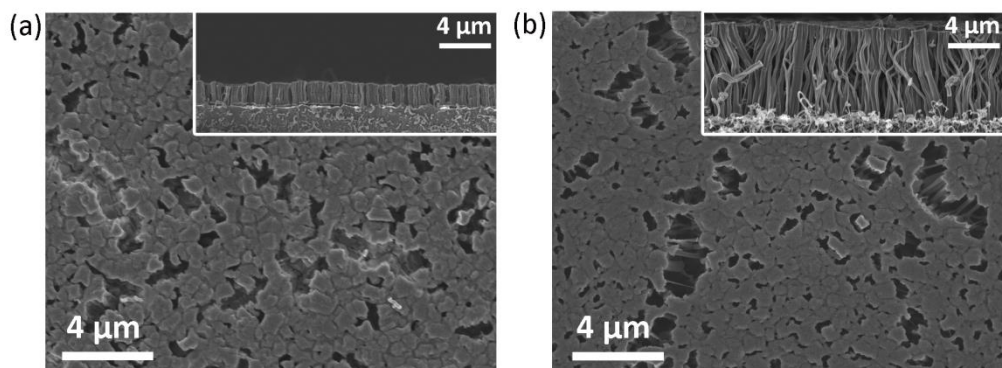


Figure S7. SEM images of the CNFs on BDD with $t_{\text{Cu,s}}$ of 60 s WOA and with growth time of CNFs for (a) 30 and (b) 120 min. The insets show their cross sections.

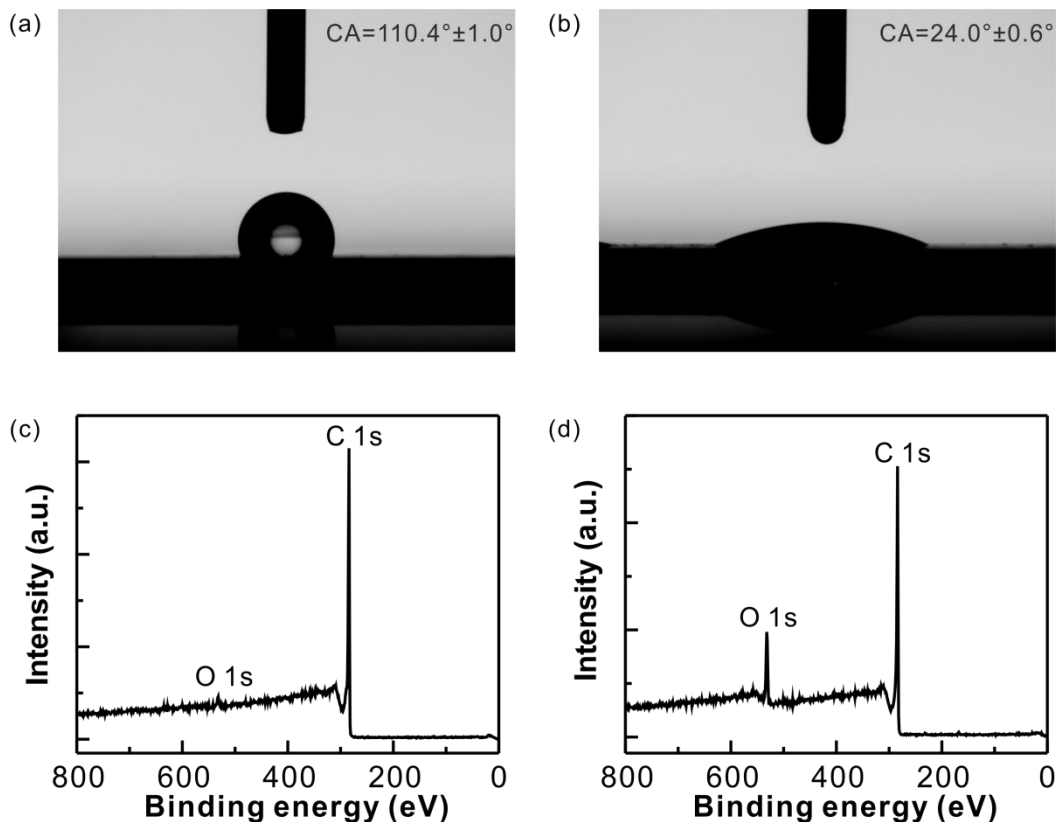


Figure S8. (a,b) Photographs of static water contact angle measurements and (c,d) XPS survey spectra of the CNFs/BDD hybrid films with $t_{\text{Cu,s}}$ of 60 s WOA (a,c) before and (b,d) after wet-chemical treatment in a mixture of concentrated sulfuric and nitric acid (v:v = 3:1) for 30 min.

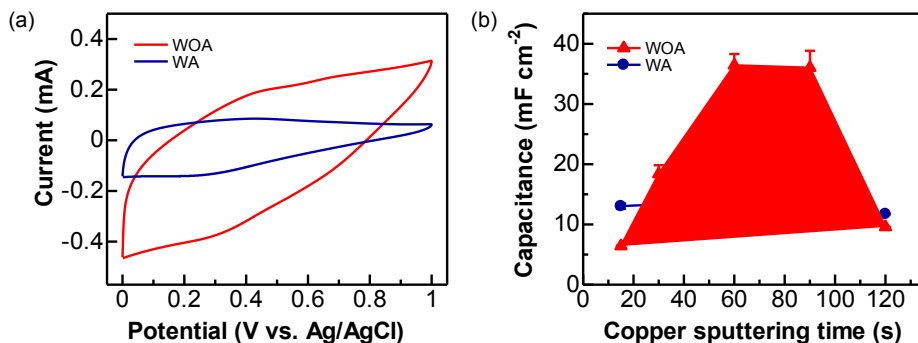


Figure S9. (a) Cyclic voltammograms of the CNFs/BDD hybrid films WA and WOA with $t_{\text{Cu,s}}$ of 60 s at a scan rate of 100 mV s⁻¹ in 1.0 M H₂SO₄ aqueous solution. (b) Comparison of the capacitances of the CNFs/BDD hybrid films with (WA) and without (WOA) annealing of Cu films with different $t_{\text{Cu,s}}$.

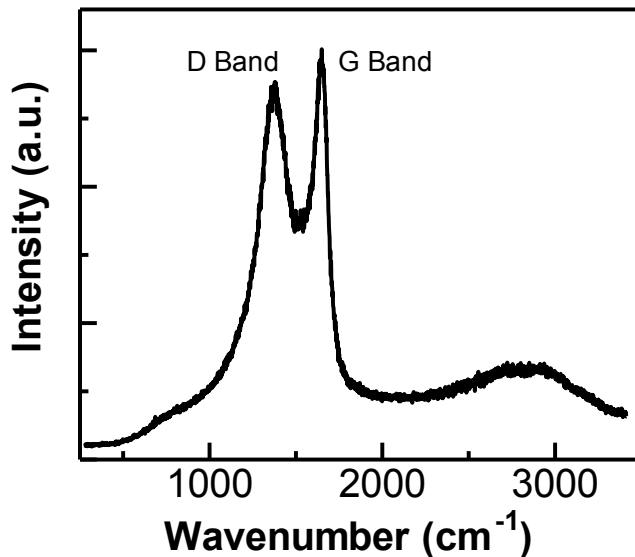


Figure S10. The Raman spectrum of a CNFs/BDD hybrid film with $t_{\text{Cu,s}}$ of 60 s WOA.

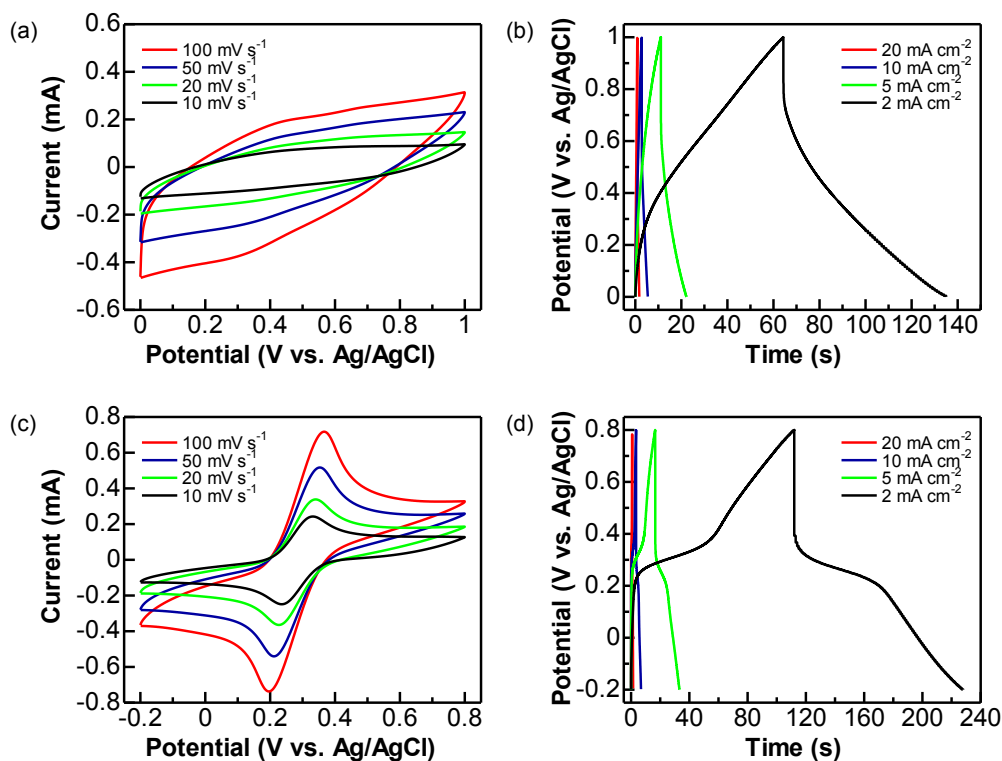


Figure S11. Performance of the CNFs/BDD supercapacitors with $t_{\text{Cu,s}}$ of 60 s WOA using a three-electrode system in (a, b) 1.0 M H_2SO_4 inert solution and (c, d) 0.05 M $\text{Fe}(\text{CN})_6^{3-/4-}$ + 1.0 M Na_2SO_4 redox electrolyte. (a, c) Cyclic voltammograms at the scan rates from 10 to 100 mV s^{-1} . (b, d) Charging-discharging curves at the current densities from 1 to 20 mA cm^{-2} .

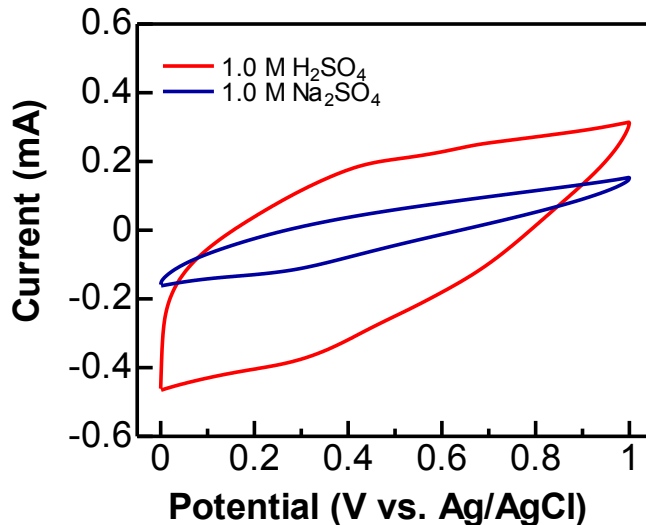


Figure S12. Cyclic voltammograms of a CNFs/BDD hybrid film with $t_{\text{Cu,s}}$ of 60 s WOA in the electrolyte of 1.0 M Na_2SO_4 and 1.0 M H_2SO_4 at a scan rate of 100 mV s^{-1} .

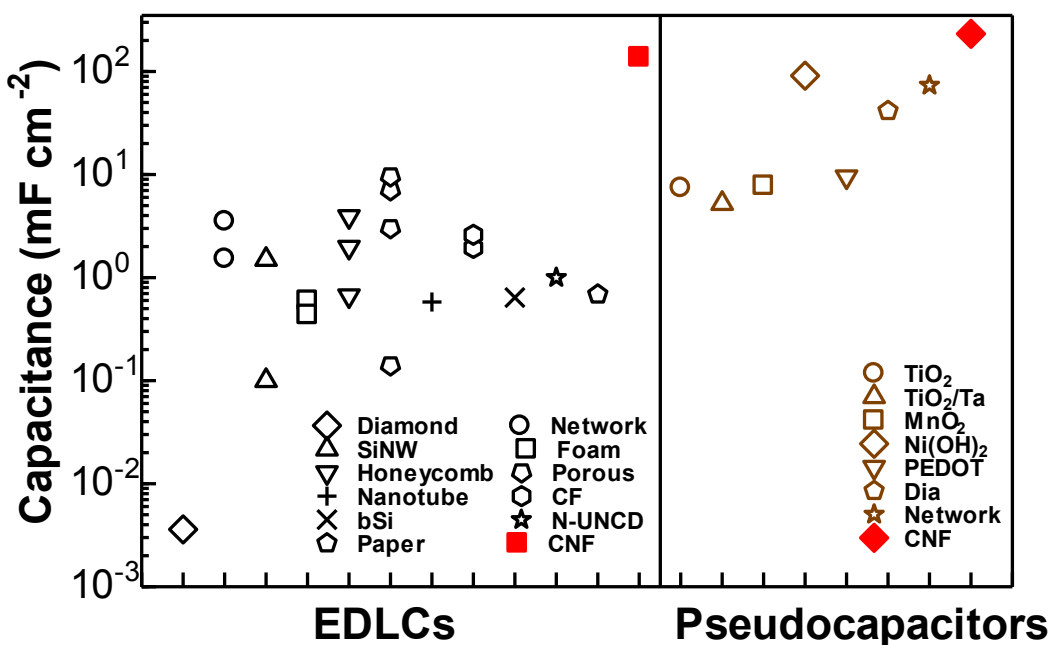


Figure S13. Comparison of the capacitance of diamond nanostructures based electric double layer capacitors (EDLCs) and pseudocapacitors (PCs) with that of diamond^[S2]. The utilized nanostructures are: diamond network (Network)^[S3], diamond/silicon nanowires (SiNW)^[S4], diamond foam (Foam)^[S5], honeycomb diamond (Honeycomb)^[S6], porous diamond (Porous)^[S7], BDD/Nanotube (Nanotube)^[S8], BDD/carbon fiber (CF)^[S9], BDD/'black silicon' (bSi)^[S10], nitrogen-included ultra-nanocrystalline diamond (N-UNCD)^[S11], diamond paper (Paper)^[S12], CNFs/BDD (CNF, this work), BDD/TiO₂ (TiO₂)^[S13], TiO₂/BDD/Ta (TiO₂/Ta)^[S14],

MnO_2/BDD ($(\text{MnO}_2)^{[\text{S}2]}$), $\text{Ni(OH)}_2/\text{Diamond}$ Nanowire ($(\text{Ni(OH})_2)^{[\text{S}15]}$), poly(3,4-(ethylenedioxy)thiophene)-coated diamond@silicon nanowires (PEDOT)^[S16]; BDD based PCs include diamond PC using redox electrolyte (Dia)^[S3a], diamond network PC using redox electrolyte (Network)^[S3a], CNFs/BDD PC using redox electrolyte (CNF, this work).

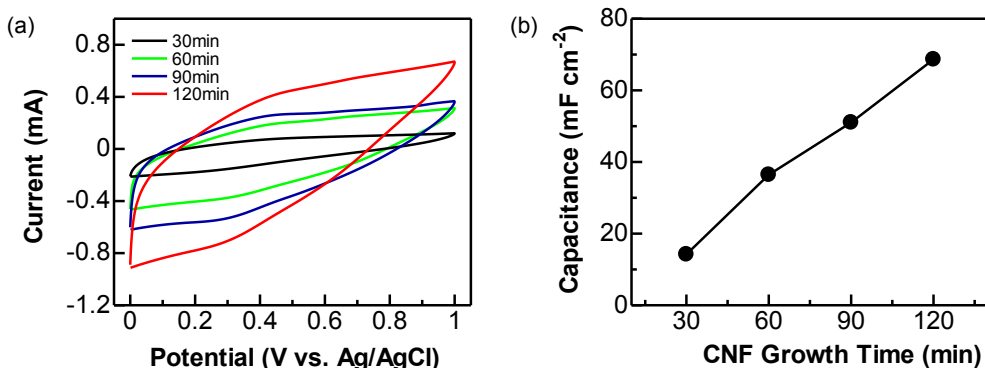


Figure S14. (a) Cyclic voltammograms of the CNFs/BDD hybrid films with $t_{\text{Cu,s}}$ of 60 s WOA with the growth time of the CNFs for 30, 60, 90, and 120 min. The scan rate is 100 mV s^{-1} and a three-electrode system is used. (b) Variation of capacitances calculated from the related CVs in (a) with the applied growth times for the CNFs.

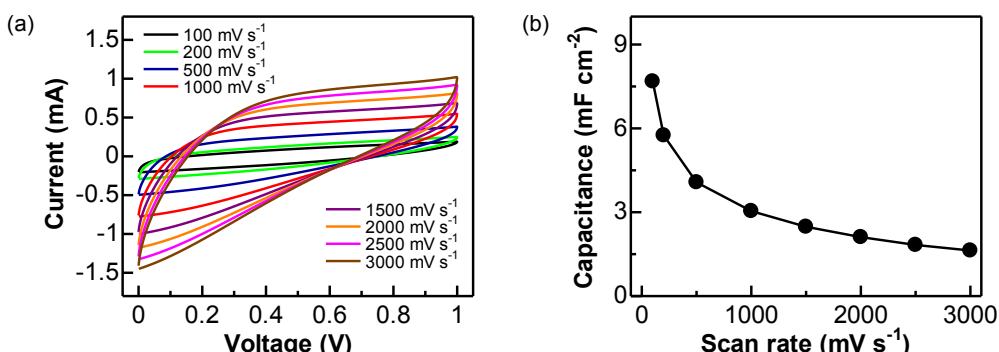


Figure S15. (a) Cyclic voltammograms of a CNFs/BDD EDLC device at the scan rates from 100 to 3000 mV s^{-1} in 1.0 M H_2SO_4 solution. (b) Variation of capacitances Calculated from the related CVs in (a) with the scan rates.

Tables**Table S1.** Comparison of the electrochemical performance of CNFs/BDD EC devices with that of other CNFs based EC devices.

	Electrode Material	Electrolyte	<i>E</i> / W h kg ⁻¹	<i>P</i> / kW kg ⁻¹	Ref.
EDLC	Hollow particle based N-doped CNF	2.0M H ₂ SO ₄	11.0	25.0	[S17]
	N,P - co-doped CNF networks	2.0 M H ₂ SO ₄	7.8	26.6	[S18]
	Cross-linked N-doped CNF network	1.0M H ₂ SO ₄	5.9	10.0	[S19]
	Mesoporous CNF	6.0 M KOH	5.1	16.0	[S20]
	CNF paper	6.0 M KOH	7.1	9.0	[S21]
	Porous CNF composites	6.0 M KOH	17.0	20.0	[S22]
PC	Porous CNF	1.0 M H ₂ SO ₄	~6.0	20.0	[S23]
	CNFs/BDD	1.0M H ₂ SO ₄	22.9	27.3	This work
	V ₂ O ₅ /CNF composites	6.0 M KOH	18.8	20.0	[S24]
	ZnO/porous activated CNF	6.0 M KOH	22.7	4.0	[S25]
PC	MnO ₂ /CNF // CNF	0.5 M Na ₂ SO ₄	36	4.4	[S26]
	CNFs/BDD	1.0M Na ₂ SO ₄ + 0.05M K ₃ Fe(CN) ₆ + 0.05M K ₄ Fe(CN) ₆	44.1	25.3	This work

Supporting References

- [S1] a) B. Zhao, X. Yan, Y. Zhou, C.-j. Liu, *Ind. Eng. Chem. Res.* **2013**, *52*, 8182; b) D. Chen, K. O. Christensen, E. Ochoa-Fernández, Z. Yu, B. Tøtdal, N. Latorre, A. Monzón, A. Holmen, *J. Catal.* **2005**, *229*, 82.
- [S2] S. Yu, N. Yang, H. Zhuang, J. Meyer, S. Mandal, O. A. Williams, I. Lilge, H. Schönherr, X. Jiang, *J. Phys. Chem. C* **2015**, *119*, 18918.
- [S3] a) S. Yu, N. Yang, H. Zhuang, S. Mandal, O. A. Williams, B. Yang, N. Huang, X. Jiang, *J. Mater. Chem. A* **2017**, *5*, 1778; b) H. Zhuang, N. Yang, H. Fu, L. Zhang, C. Wang, N. Huang, X. Jiang, *ACS Appl. Mater. Interfaces* **2015**, *7*, 5384.
- [S4] a) F. Gao, G. Lewes-Malandrakis, M. T. Wolfer, W. Müller-Sebert, P. Gentile, D. Aradilla, T. Schubert, C. E. Nebel, *Diamond Relat. Mater.* **2015**, *51*, 1; b) D. Aradilla, F. Gao, G. Lewes-Malandrakis, W. Müller-Sebert, D. Gaboriau, P. Gentile, B. Iliev, T. Schubert, S. Sadki, G. Bidan, C. E. Nebel, *Electrochim. Commun.* **2016**, *63*, 34.
- [S5] F. Gao, M. T. Wolfer, C. E. Nebel, *Carbon* **2014**, *80*, 833.
- [S6] a) K. Honda, T. N. Rao, D. A. Tryk, A. Fujishima, M. Watanabe, K. Yasui, H. Masuda, *J. Electrochem. Soc.* **2000**, *147*, 659; b) K. Honda, T. N. Rao, D. A. Tryk, A. Fujishima, M. Watanabe, K. Yasui, H. Masuda, *J. Electrochem. Soc.* **2001**, *148*, A668; c) M. Yoshimura, K. Honda, R. Uchikado, T. Kondo, T. N. Rao, D. A. Tryk, A. Fujishima, Y. Sakamoto, K. Yasui, H. Masuda, *Diamond Relat. Mater.* **2001**, *10*, 620.
- [S7] a) C. Hébert, E. Scorsone, M. Mermoux, P. Bergonzo, *Carbon* **2015**, *90*, 102; b) C. Shi, C. Li, M. Li, H. Li, W. Dai, Y. Wu, B. Yang, *Appl. Surf. Sci.* **2016**, *360*, Part A, 315; c) T. Kondo, Y. Kodama, S. Ikezoe, K. Yajima, T. Aikawa, M. Yuasa, *Carbon* **2014**, *77*, 783; d) V. Petrák, Z. Vlčková Živcová, H. Krýsová, O. Frank, A. Zukal, L. Klimša, J. Kopeček, A. Taylor, L. Kavan, V. Mortet, *Carbon* **2017**, *114*, 457.
- [S8] C. Hébert, J. P. Mazellier, E. Scorsone, M. Mermoux, P. Bergonzo, *Carbon* **2014**, *71*, 27.

- [S9] a) E. C. Almeida, A. F. Azevedo, M. R. Baldan, N. A. Braga, J. M. Rosolen, N. G. Ferreira, *Chem. Phys. Lett.* **2007**, *438*, 47; b) E. C. Almeida, M. R. Baldan, J. M. Rosolen, N. G. Ferreira, *Diamond Relat. Mater.* **2008**, *17*, 1529.
- [S10] P. W. May, M. Clegg, T. A. Silva, H. Zanin, O. Fatibello-Filho, V. Celorio, D. J. Fermin, C. C. Welch, G. Hazell, L. Fisher, A. Nobbs, B. Su, *J. Mater. Chem. B* **2016**, *4*, 5737.
- [S11] W. Tong, K. Fox, A. Zamani, A. M. Turnley, K. Ganesan, A. Ahnood, R. Cicione, H. Meffin, S. Prawer, A. Stacey, D. J. Garrett, *Biomaterials* **2016**, *104*, 32.
- [S12] F. Gao, C. E. Nebel, *ACS Appl. Mater. Interfaces* **2016**, *8*, 28244.
- [S13] a) M. Sawczak, M. Sobaszek, K. Siuzdak, J. Ryl, R. Bogdanowicz, K. Darowicki, M. Gazda, A. Cenian, *J. Electrochem. Soc.* **2015**, *162*, A2085; b) K. Siuzdak, R. Bogdanowicz, M. Sawczak, M. Sobaszek, *Nanoscale* **2015**, *7*, 551; c) M. Sobaszek, K. Siuzdak, M. Sawczak, J. Ryl, R. Bogdanowicz, *Thin Solid Films* **2016**, *601*, 35.
- [S14] C. Shi, H. Li, C. Li, M. Li, C. Qu, B. Yang, *Appl. Surf. Sci.* **2015**, *357*, Part B, 1380.
- [S15] F. Gao, C. E. Nebel, *Phys. Status Solidi A* **2015**, *212*, 2533.
- [S16] D. Aradilla, F. Gao, G. L. Malandrakis, W. Müller-Sebert, P. Gentile, M. Boniface, D. Aldakov, B. Iliev, T. J. S. Schubert, C. E. Nebel, G. M. Bidan, *ACS Appl. Mater. Interfaces* **2016**, *8*, 18069.
- [S17] L.-F. Chen, Y. Lu, L. Yu, X. W. Lou, *Energy Environ. Sci.* **2017**, *10*, 1777.
- [S18] L.-F. Chen, Z.-H. Huang, H.-W. Liang, H.-L. Gao, S.-H. Yu, *Adv. Funct. Mater.* **2014**, *24*, 5104.
- [S19] Y. Cheng, L. Huang, X. Xiao, B. Yao, L. Yuan, T. Li, Z. Hu, B. Wang, J. Wan, J. Zhou, *Nano Energy* **2015**, *15*, 66.
- [S20] Z. Liu, D. Fu, F. Liu, G. Han, C. Liu, Y. Chang, Y. Xiao, M. Li, S. Li, *Carbon* **2014**, *70*, 295.
- [S21] C. Ma, Y. Li, J. Shi, Y. Song, L. Liu, *Chem. Eng. J.* **2014**, *249*, 216.

- [S22] B.-H. Kim, K. S. Yang, H.-G. Woo, K. Oshida, *Synth. Met.* **2011**, *161*, 1211.
- [S23] C. Tran, V. Kalra, *J. Power Sources* **2013**, *235*, 289.
- [S24] B.-H. Kim, C. H. Kim, K. S. Yang, A. Rahy, D. J. Yang, *Electrochim. Acta* **2012**, *83*, 335.
- [S25] C. H. Kim, B.-H. Kim, *J. Power Sources* **2015**, *274*, 512.
- [S26] C.-F. Zhao, K. Lu, H. Ma, *RSC Adv.* **2016**, *6*, 107638.